

Experimental Study of Asphaltene Deposition in Transparent Microchannels

Using Light Absorption Method

Y. Zhuang¹, A. Goharzadeh^{1*}, Y. J. Lin², Y. F. Yap¹, J. C. Chai³, N. Mathew⁴, F. Vargas², Sibani L. Biswal²

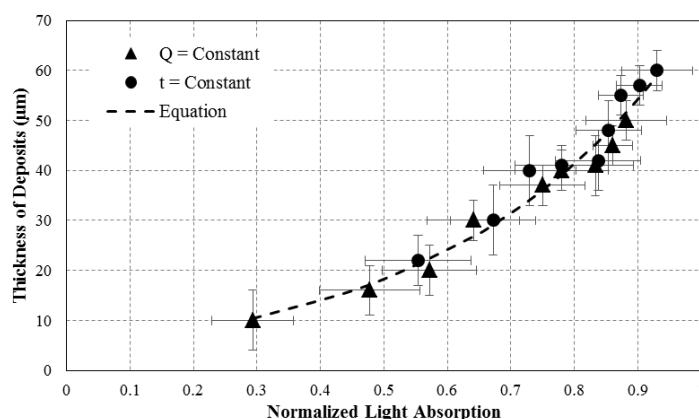
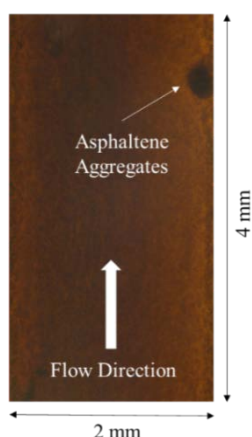
¹Department of Mechanical Engineering, The Petroleum Institute, Abu Dhabi, UAE,

²Department of Chemical and Biomolecular Engineering, Rice University, TX, USA,

³School of Computing & Engineering, University of Huddersfield, Huddersfield, UK,

⁴Department of Chemical Engineering, The Petroleum Institute, Abu Dhabi, UAE.

GRAPHICAL ABSTRACT



Correlation between deposition thickness and normalized light absorption

Heptane-induced asphaltene precipitation from crude oil and its deposition in a vertical transparent microchannel is investigated. The amount of asphaltene deposited on a transparent channel wall is quantified using a non-intrusive flow visualization technique based on reflected light intensity and image analysis. Asphaltene deposits strongly affect the reflected light intensity through the change of mixture color in the recorded images. An empirical equation is developed to correlate the intensity of the light absorption to the thickness of the deposited asphaltene in a transparent microchannel. Non-uniform deposition along the longitudinal direction of the microchannel is also characterized.

Key words:

Asphaltene Deposition; Micro-channels; Light Absorption Method; Non-uniform Deposits; Image Processing

1. Introduction

In the process of oil production, transportation and refinery, asphaltene deposition is a recurring problem, especially for wide utilization of enhanced oil recovery (EOR) technologies. Deposition of precipitated asphaltene particles can occur in both primary^[1] and secondary^[2] production and causes formation damage in reservoirs, blockage in wellbores or even problem in separators, pumps, pipelines, heat exchangers and various equipment.^[3] Removal of asphaltene deposition can cost between \$0.5 to 3 MM U.S.^[4] It is therefore critical to understand the deposition process for devising effective mitigation procedures. One strategy to characterize asphaltene deposition would be to induce and deposit asphaltene particles in micro-channels^[5] where the effect of interfacial properties and intrinsic asphaltene behaviors can be investigated. In previous experimental studies, both stainless steel capillary tubes^[6-10] and transparent glass capillary tubes or micro-channels^[11-20] have been largely employed to visualize the process of asphaltene deposition. A detailed summary of experimental conditions has been presented in our previous study.^[21]

Hoepfner *et al.*^[10] conducted a series of experiments in metal capillaries having a mixing flow of heptane and crude oil. They have visualized the highly non-uniform axial deposit profile using scanning electron microscope (SEM), and found that the pressure drop increased with increasing elapsed time during the flow tests. Seifried *et al.*^[11] used a rectangular glass capillary to visualize the asphaltene deposition. They suggested that the asphaltene deposition rate was sensitive to the magnitude of the average mixture velocity at the earlier experimental time. This early asphaltene

behavior relied on the flux of particles through the experimental setup. They also found that the influence of flow rate on deposition thickness was almost negligible. Boek *et al.*^[12-14] conducted asphaltene deposition in a rectangular glass capillary and shows the significance of colloidal interaction potentials. They also investigated the influence of precipitant fraction and total volumetric flow rate on pressure drop and found that more asphaltene was deposited in the inlet of the capillary tube.^[14] The influence of water-alternating-solvent (WAS) injection process on asphaltene deposition was studied by Dehghan *et al.*^[15] The microscopic pictures of asphaltene precipitate were visualized in glass micro-porous models. They have observed that the solvent injection could produce precipitated asphaltene particles in localized entrapped regions where the oil was stagnant. Lawal *et al.*^[16] investigated the thickness of asphaltene deposits via imaging the micro-capillary tubes combined with pressure drop measurements. They observed uniform deposition in the capillary tube and the deposition was independent of flow. Asphaltene aggregates presenting chainlike structures were observed. Using transparent glass capillary tube and micrographs, they studied the morphology of asphaltene aggregates. Hu *et al.*^[17] investigated the asphaltene deposition inside a transparent packed-bed micro-reactor (μ PBR) using a CCD camera. They observed a uniform color change in the microchannel for different pore volume with no obvious channeling. They observed that asphaltene deposition decreased with increasing Reynolds number. Doryani *et al.*^[18] studied asphaltene precipitation and deposition in a uniformly patterned glass micromodel. Their observation was based on the color of oil phase changing from black to grey due to loss of dissolved dark asphaltenes, as soon as precipitation took place. Lin *et al.*^[19] investigated the dynamic growth of asphaltene deposition at pore scale using microfluidic devices. With the visualization technique, the convection-diffusion effect on the deposition growth rate and dynamic alteration of the morphology were observed. Zanganeh

et al.^[20] used high-pressure visual cell to characterize asphaltene deposition process during CO₂ miscible injection into oil reservoirs. They observed that the asphaltene deposition rate depends strongly on the pressure and CO₂ increases asphaltene deposition in all the pressure ranges comparing to the case of natural depletion.

Previous experimental studies, presented above, express the importance of light absorption from deposited asphaltenes. However an empirical correlation connecting the intensity of the reflected light from a deposit layer to its thickness has not been provided yet. Present study undertakes an experimental work to fill this gap by investigating the relationship between the light intensity emitted from asphaltene deposits and their thickness.

This study is focused on a non-intrusive method of measurement to quantify the amount of asphaltene deposits in a microchannel. The light absorption technique is used to quantify the amount of asphaltene deposits. Experimental setup and measurement method are presented in the next section. Measurements are validated with a concomitant method based on 3D measurement of the deposition presented on our previous work^[21]. Influence of different crude oil to n-heptane ratios and flow rates on asphaltene deposition are presented. Finally, spatial characteristics of the asphaltene deposition along the micro-channel are presented in the last section of this paper.

2. Experimental Setup and Measurement Methods

2.1 Experimental Setup

The experimental setup consists of a vertical transparent microchannel, a dual syringe pump with two glass syringes, a collection tank and a microscope for flow visualization. The microchannel was fabricated from Plexiglas and has the characteristics depth of 250 μm and rectangular area of 50 mm Length \times 2 mm Width. In this experiment the flow direction is from bottom to top. The working fluids are crude oil and n-heptane. Crude oil and n-heptane are stored

in two separate glass syringes (SAMCO, 10 ml). The glass syringes are connected using transparent plastic tubes to a T-junction where mixing of crude oil and n-heptane occur. The mixture then flows into the microchannel. A syringe pump (Cole-Parmer with 140 mL/min maximum flow rate) is used to control and drive the working fluids. The ratio of crude oil and n-heptane is controlled by the syringe pump. All experiments were conducted using a fixed injection ratio of crude oil : n-heptane (3:7). The range of flow rates used was between 0.003 to 0.008 ml/min while the experimental elapsed times from 4 to 14 hours were examined. The experimental schematic and setup for vertical configuration are shown in Figure 1.

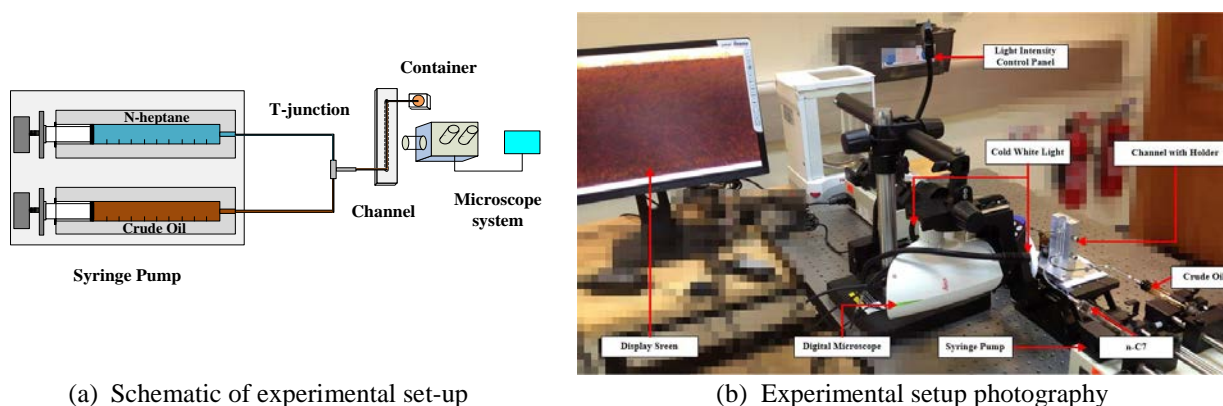


Fig. 1. Experimental setup for vertical configuration

2.2 Crude oil preparation

A detailed preparation of crude oil, used in this experiment, is reported by Zhuang *et al.* [21] Before the experiment, crude oil was centrifuged for 15 minutes at 4000 rpm. The supernatant was analyzed by microscope (Hirox 3D digital microscope KH-7700) and the analysis results indicated no obvious existence of suspended asphaltene particles. The centrifuged crude oil was used in the experiment. The microscope was used to capture high resolution images. The temperature of the working fluids is maintained at a constant temperature of 24°C. All experimental values illustrated in results sections represent average values of at least three experiments for error quantification. Properties of the crude oil, obtained from SARA analysis

were reported in Table 1. The determination of various components in the crude oil such as Saturates, Aromatics and Resins were characterized by using ASTM D-2007m method and the Asphaltene component was characterized by IP 143 method. The n-heptane precipitant has a density and kinematic viscosity of 0.684 g/cm³ and 0.647 cSt, respectively. Both density and kinematic viscosity of the crude oil were measured by ASTM D-4052 and ASTM D-445, respectively.

Table 1. Properties of crude oil obtained from SARA analysis

| °API | Density at 20°C (g/cm ³) | Kinematic Viscosity (cSt) | Saturates (Wt. %) | Aromatics (Wt. %) | Resins (Wt. %) | Asphaltenes (Wt. %) |
|------|---|---------------------------------|----------------------|----------------------|-------------------|------------------------|
| 36.5 | 0.8412 | 6.505 | 49.9 | 14.2 | 5.6 | 0.4 |

2.3 Image Processing Method

During the experiments, the positions of the micro-channel and microscope were fixed. The LEICA DMS300 microscope, having a 0.8× lens with a 6× magnification, records images at the center of the microchannel. The recoded image has a fixed rectangular size of 2 × 4 mm². Two methods of measurements are used in this experiment (i) dynamic technique which is based on recording image while the fluid mixture is flowing in the micro-channel and (ii) static technique where the fluid mixture is removed from the test section before recording the images.

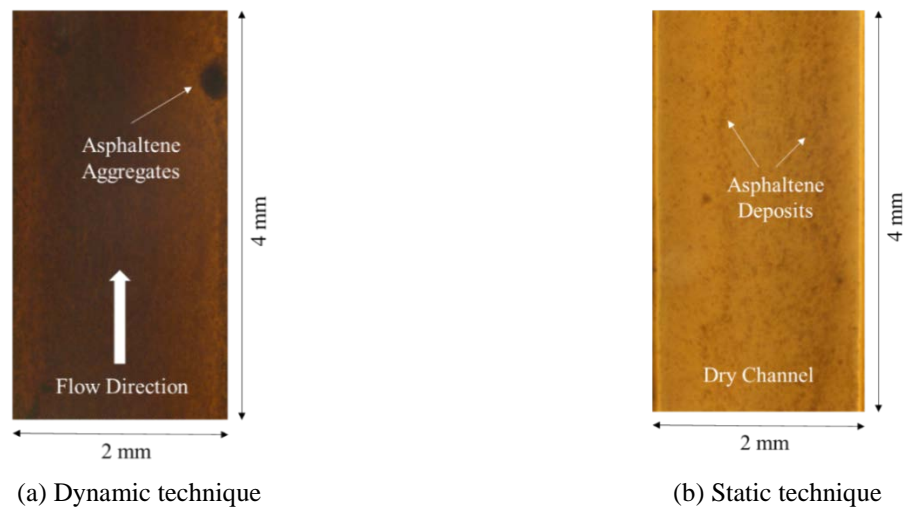


Fig. 2. Experimental images in terms of dynamic and static technique

The dynamic technique focuses on combined aggregation and deposition phenomena (see Fig. 2a). Asphaltene aggregates are characterized by large and dark region flowing in the microchannel. The static technique focuses only on the deposition phenomena inside the microchannel (see Fig. 2b). The asphaltene deposits, captured in Figure 2b, are characterized by small and dark spot distributed uniformly in the image. Uniform asphaltene deposition can be easily quantified to an average pixel value. Figures 3a and 3c represent color images taken after 4 hours and 12 hours, respectively. In Fig. 3 3a, the uniform light brown color is due to the presence of residue mixture (crude oil + n-heptane) in the microchannel. Since asphaltene particles are darker than oil, the image becomes darker wherever asphaltene is deposited. Dark spots appearing uniformly in the image represent asphaltene deposits. In Figure 3c the entire image is covered with asphaltene and the image is uniformly dark. Therefore, the distinction of asphaltene deposition in the test section can be recognized and quantified accordingly.

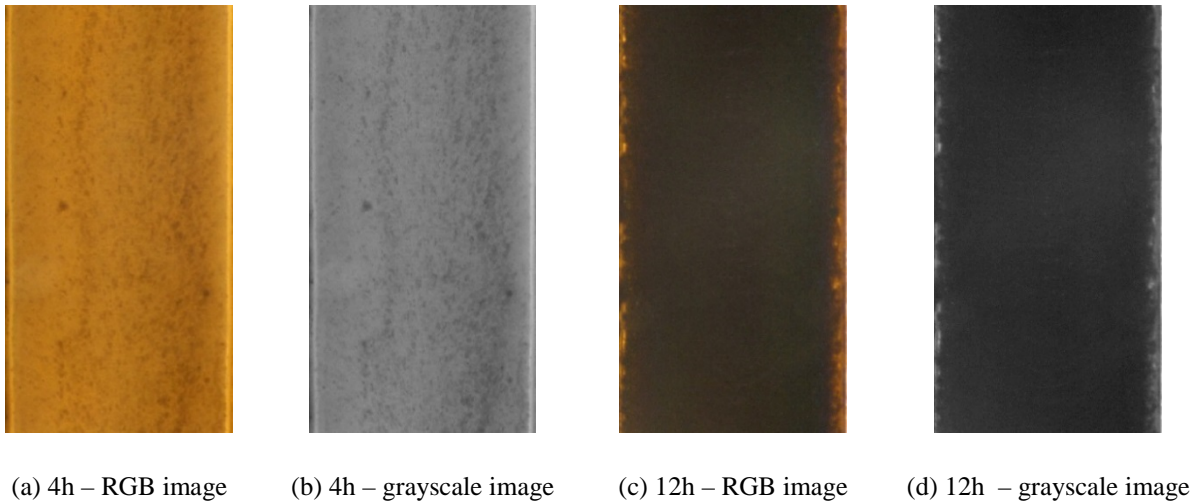


Fig. 3. Color (RGB) and grayscale images of dried micro-channels - Ratio 3:7

Image analysis was conducted via MATLAB program to interpret experimental images. The obtained images shown in Figures 3a and 3c were converted to grayscale images illustrated in Figures 3b and 3d, respectively. Pixel value of grayscale images ranges from 0 (black) to 255

(white). Histogram of grayscale images are shown in Figure 4. Pixel value centers around 128 for Figure 3b and 52 for Figure 3d, respectively. Higher pixel value represents less deposit. Through the analysis of several experimental images, a pixel value of 128 is taken as the threshold of zero deposit thickness in the presence of mixture residue. The pixel value decreases with increasing deposit thickness and reaches a minimum value of 38 when the deposit is thickest. These two values are estimated and representative of the current laboratory conditions. Using the threshold value of 128, the accuracy of image processing can be improved. An average pixel value of each image is calculated since the asphaltene deposition is approximately uniform in the focused area. Then, for ease of quantification, the pixel value is used to calculate the normalized light absorption ranging from 0 (no deposit, i.e. a pixel value of 128) to 1 (full deposit, i.e. a pixel value of 38).

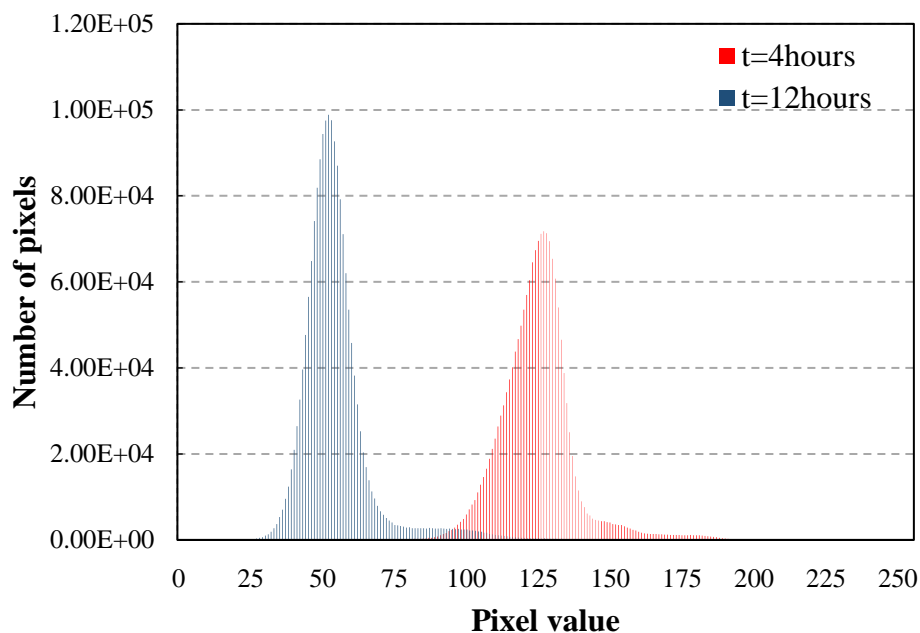


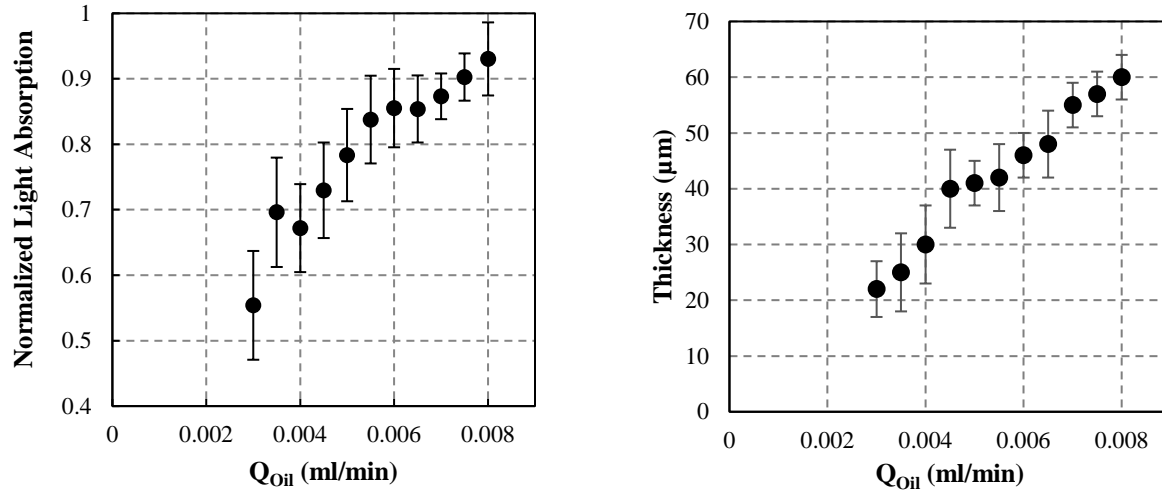
Fig. 4. Histogram of 4 hrs and 12 hrs experimental images

Experiments for different elapsed time were each repeated for more than three times. The flow rate of n-heptane can be calculated from the ratio of crude oil to n-heptane which is 3:7.

After experiments, microchannels were stored in laboratory conditions until they were completely dried (24 hours). This can be observed visually from the microscope. Microchannels were then opened mechanically. Subsequently, the thickness of asphaltene deposits can be measured by 3D digital microscope.^[21] All measurements were performed at the test section, located in the middle of the channel and 25 mm away from the inlet.

3. Experimental Results

With increasing asphaltene deposits along the channel, the recorded image becomes darker. In this section, the correlation between deposition thickness and normalized light absorption is under investigation. Two sets of measurement are compared (i) the behavior of asphaltene deposition changes in a small range of flow rate of crude oil and (ii) the evolution of asphaltene deposition with time for a constant flow rate of crude oil. Normalized light absorption for different flow rates of crude oil is presented Figure 5-a. The corresponding evolution of asphaltene deposition thickness for the same microchannel is measured using the 3D microscopy and presented in Figure 5b. For both Figures 5a and 5b, the flow rate of crude oil ranges from 0.003 to 0.008 ml/min with a 0.0005 ml/min flow rate interval. It is observed that both the thickness of asphaltene deposits and normalized light absorption increases continuously with increasing flow rate. The amount of asphaltene deposits for $Q_{oil} < 0.003$ ml/min is very small and therefore very difficult to be measured.



(a) Normalized light absorption

(b) Thickness of deposits

Fig. 5. Asphaltene deposition in terms of flow rate at constant elapsed time ($\Delta T=10$ hours)

Asphaltene deposition depends also strongly on the elapsed time for a constant flowrate. The amount of asphaltene deposits quantified as a function of elapsed time is illustrated in Figure 6. Figure 6a shows measured normalized light absorption variation versus time and Figure 6b illustrates the corresponding thickness of deposited asphaltene measured by a 3D microscope. ^[21] For both Figures 6a and 6b, the time period ranges from 4 to 14 hours with a 1 hour time interval. It is observed that the amount of asphaltene deposits grows continuously in the microchannel reaching a thickness of 50 μm at elapsed time of 14 hours. The corresponding normalized light absorption is reaching a saturated value of 0.9 after 14 hours, showing that beyond this time the asphaltene deposits cannot be quantified by the light absorption method. Finally, the amount of asphaltene deposits for the first 3 hours is very small and therefore very difficult to be measured.

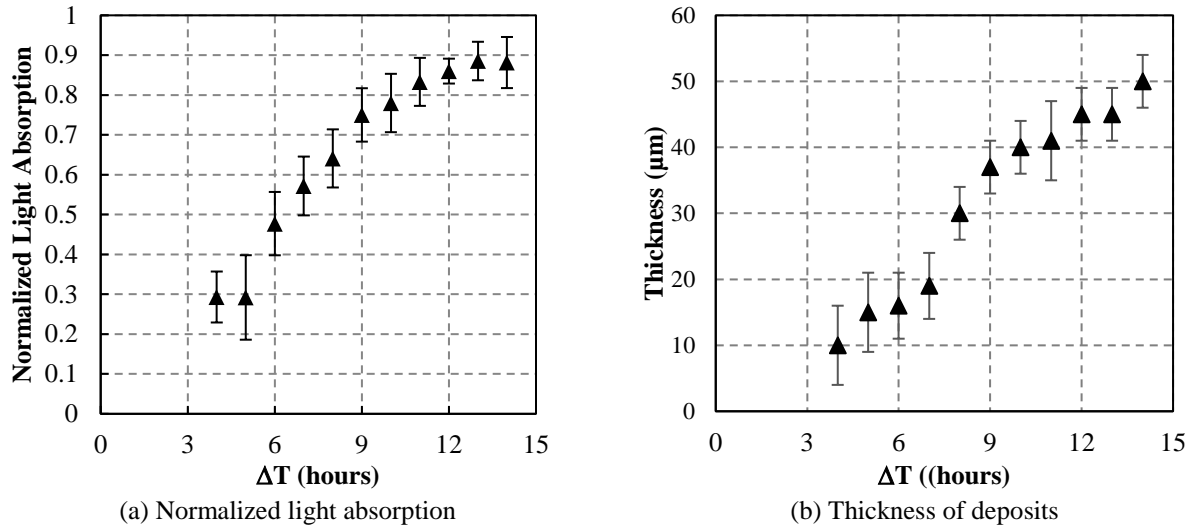


Fig. 6. Asphaltene deposition in terms of elapsed time for constant flow rate ($Q_{oil}=0.005$ ml/min)

As mentioned above, measurements of both normalized light absorption and 3D digital microscopy were performed at the same location, i.e. the middle of the microchannel. By combining the mentioned methods, a relation between them can be obtained. Figure 7 presents two experimental data including constant flow rate (0.005 ml/min) and constant time period (10 hours). The correlation between deposit thickness and normalized light absorption is consistent for these two different experiments.

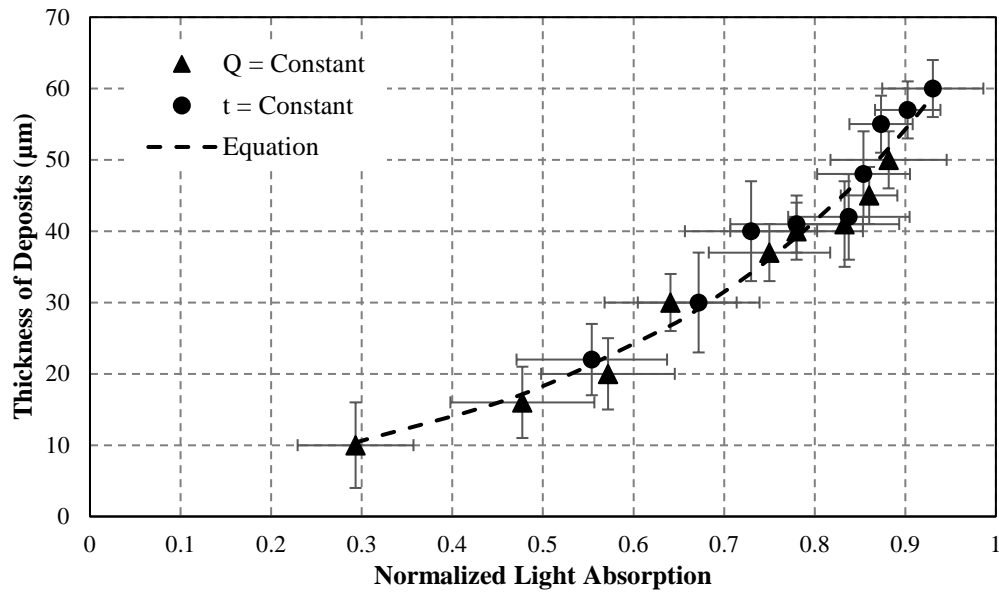


Fig. 7. Correlation between deposition thickness and normalized light absorption

Based on the experimental results showed in Figure 7, the average correlation function can be obtained and it is close to the exponential equation.

$$\delta(I) = 4.66e^{2.73I} \quad (3)$$

In Equation 3, normalized light absorption represents quantitatively the thickness of asphaltene deposits. Furthermore, deposition thickness can be calculated from normalized light.

3.1 Validation of the Correlation Equation

Experiments were performed at constant injection volume of crude oil (3 ml) with a higher range of flow rate from 0.005 to 0.05 ml/min with a 0.005 ml/min interval. The ratio of crude oil to n-heptane is fixed at 3:7. As illustrated in Figure 8, asphaltene deposits reflected by normalized light absorption reduce with the increase of flow rate. The change of flow rate leads to the change of residence time. With the increase of flow rate, residence time reduces from 90 s at 0.005 ml/min to 9 s at 0.05 ml/min. Normalized light absorption changes from near 0.8 at 0.005 ml/min to 0.15 when the flow rate is 10 times of the lowest flow rate. This result can be easily fitted by a linear equation as the follow.

$$I(Q_{oil}) = -14.78Q_{oil} + 0.87 \quad (4)$$

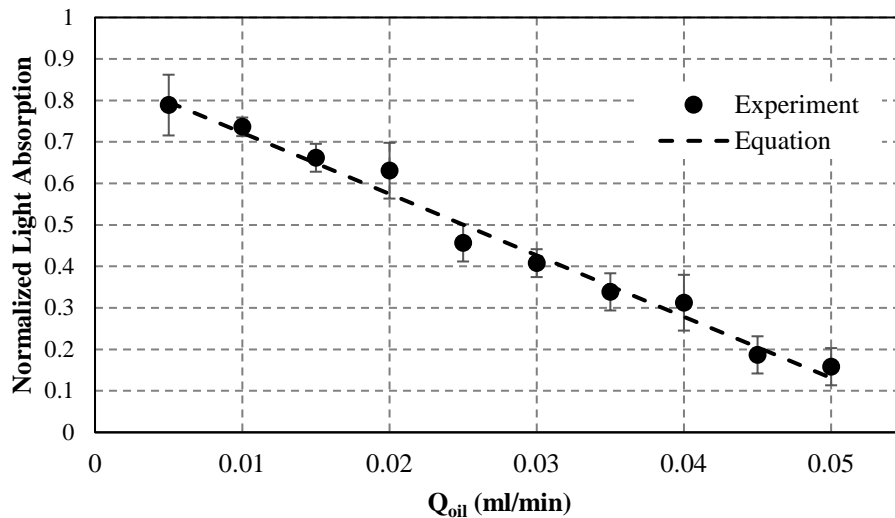


Fig. 8. Normalized light absorption as a function of flow rate at constant injection volume (3 ml) in microchannel

A thickness calculation is also conducted using Equation 3 for validation. Both measured and calculated thickness of the asphaltene deposits are compared in Figure 9. It can be observed that the correlation predicts the thickness of the asphaltene deposits reasonably well.

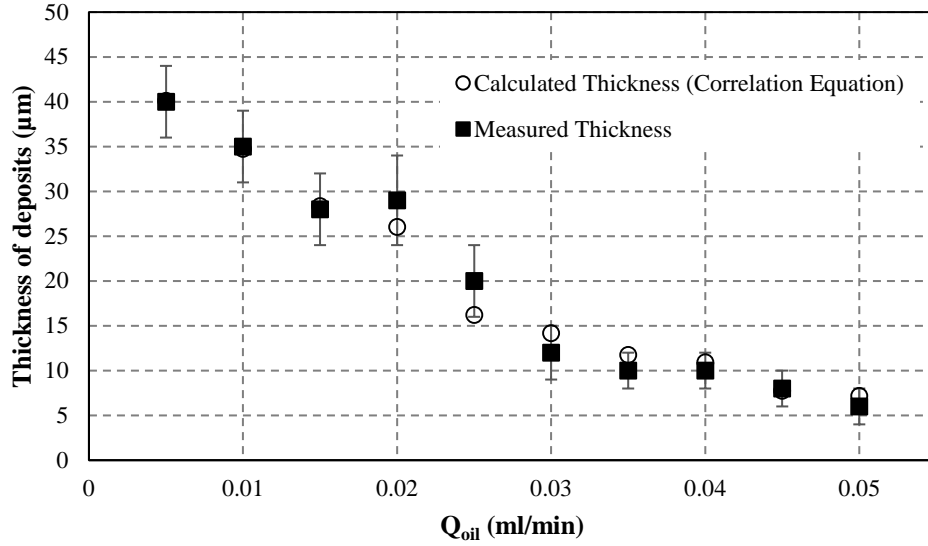


Fig. 9. Calculated thickness versus measured thickness

Deposition process of asphaltene is often accompanied by significant erosion induced by the dominance of shear force on the deposition.^[6] This result also shows the effect of shear forces on the asphaltene deposition and this range of shear rate is within the shear limited regime. Increasing flow rate leads to a higher shear rate and therefore transports asphaltene particles fast without depositing on the surface. Besides, the higher shear force removes deposited asphaltene back into the solution. Shear rate can be calculated using the equation 5. ^[22]

$$\gamma_{average} = \frac{3Q_{total}}{8a^2b} \quad (5)$$

where, a is half of the depth of microchannel and b is half of the width of the microchannel.

Figure 10 illustrates the relation of normalized light absorption and the calculated shear rate. The fitted curve is given by equation 6:

$$I(\gamma) = -0.011\gamma + 0.87 \quad (6)$$

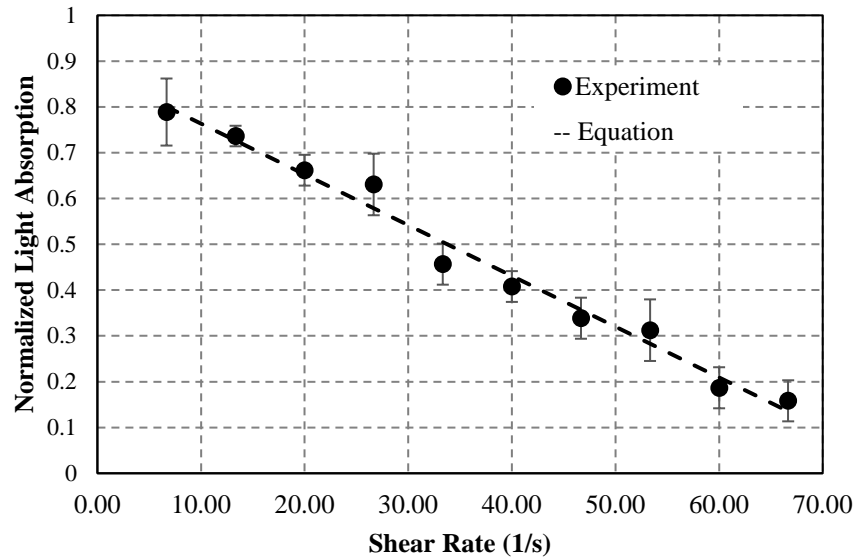


Fig. 10. Normalized light absorption as a function of shear rate

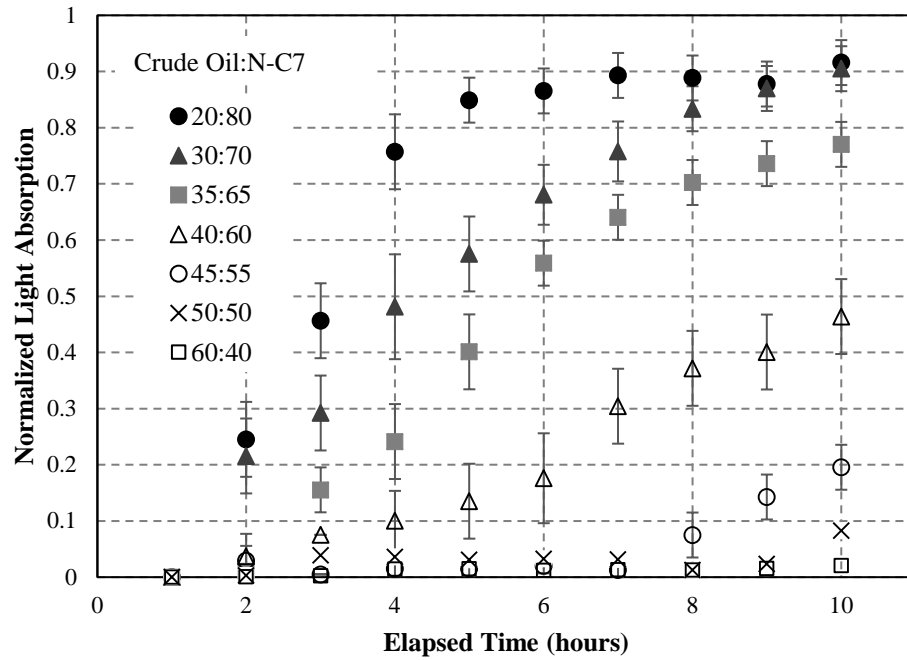
3.2 Influence of Injection Ratio on Asphaltene Deposition

In this section, the influence of injection ratio on asphaltene deposition is studied. The flow rate of n-heptane was calculated using the ratio 3:7 corresponding to a crude oil and n-heptane flowrate of $Q_{oil} = 0.005\text{ml/min}$ and $Q_{n-C7} = 0.0117\text{ml/min}$, respectively. Total injection time was 10 hours for all experiments and images were recorded every one hour using a dynamic technique. The ratio of crude oil to n-heptane varies from a low ratio of 6:4 to a high ratio of 2:8.

Figure 11a shows that asphaltene deposits increase with increasing mixture fluid ratio and elapsed time. It is observed that the time of initial deposition becomes shorter with the increase of the mixture ratio. For a ratio of 6:4, no deposit is observed in the whole channel even after 10 hours of continuous injection. This result indicates that the onset of precipitation for this crude oil is higher than 40% of n-heptane. As the ratio of n-heptane increases, asphaltene deposit appears earlier in the system. When the n-heptane concentration is between 40% and 55%, the asphaltene deposition rate is negligible during first 8 hours and significantly increases after 8 hours. For the ratio of n-heptane higher than 60%, asphaltene deposits rapidly in the system,

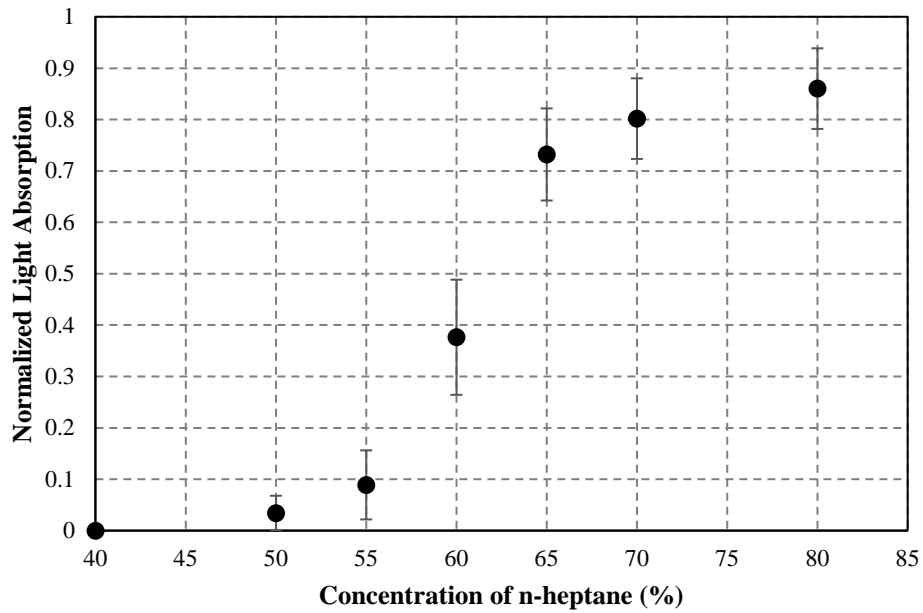
between 3 and 7 hours. After 7 hours, the rate of the deposition decreases in the system reached a corresponding constant normalized light absorption value of 0.9.

It can be observed that the deposition process consists of three stages. Firstly, small asphaltene particles deposit on the surface of the microchannel. Since the surface is larger compared to the size of asphaltene, this stage is slow and results in a slow deposition rate. Deposited asphaltene particles form obstacles to prevent more asphaltene particles from flowing, and therefore the second stage of this process is characterized by a rapid and continuous increase of the deposits. Finally, the deposition rate decreases in the system due to the size limitation of the microchannel, flowrate change or surface conditions. Figure 11-b illustrates the effect of n-heptane concentration on asphaltene deposition. These experimental results are obtained by using the static technique where the channel is dried before recoding images. It is clear that the deposit amount increases with increasing mixture ratio from 40% to 80%. The deposition rate is almost negligible for n-heptane concentration less than 50%. For n-heptane concentration higher than 55%, the amount of asphaltene deposits increases significantly. The corresponding normalized light absorption changes from 0.1 to 0.8 when the concentration range is increased from 55% to 70%. For high n-heptane concentration (>70%) the asphaltene deposits reach a constant value corresponding to a normalized light absorption of 0.9.



(a) Asphaltene aggregation and deposition vs time for different mixture ratio

Note: the ratio is crude oil to n-C7.



(b) Asphaltene deposition vs concentration of n-C7

Fig. 11. The effect of injection ratio of crude oil and n-C7 on asphaltene deposition

3.3 Non-Uniform Distribution of Asphaltene Deposition

Image processing method in section 2.2 was performed for a fixed area located at the middle of the channel. The captured images show that the asphaltene deposition in this selected area is uniform. However, when it comes to the entire microchannel, the deposit amount is approximately decreasing from inlet to outlet. To quantify the deposits along the longitudinal direction, image processing was applied. The average pixels at any longitudinal direction (y direction) can be calculated using a MATLAB program. After that, all obtained values are inversed by subtraction of 255 to indicate that darker value stands for deposition.

Figure 12 shows the gradient of light absorption along the longitudinal axis of the channel having a total length of 48 mm. The measurements were performed for four different duration ranging between 4 to 14 hours. The value of light absorption is actually the inversed pixel value ($255 - \text{real pixel}$). Different color curves represent different time ranging from 4 to 14 hours with a 4-hour interval. All experiments are conducted using the same flow rate of crude oil and n-heptane, with 0.005 ml/min and 0.0117 ml/min (3:7 ratio), respectively. From the figure, it is clear that deposition is decreasing along the flow direction without considering the inlet and outlet effect. The maximum deposition is located near 5 mm away from the inlet. The position of the maximum asphaltene deposition does not depend on elapsed time experiment.

Figure 13 illustrates the deposition along the longitudinal direction for different flow rate of crude oil. A similar trend can be found in all curves where asphaltene deposition declines with increasing longitudinal distance. The maximum deposition position is located near 5 mm distance away from the inlet. However, it is shifted downstream when the flow rate is higher, such as 0.008 ml/min. Asphaltene deposition grows with increasing flow rate.

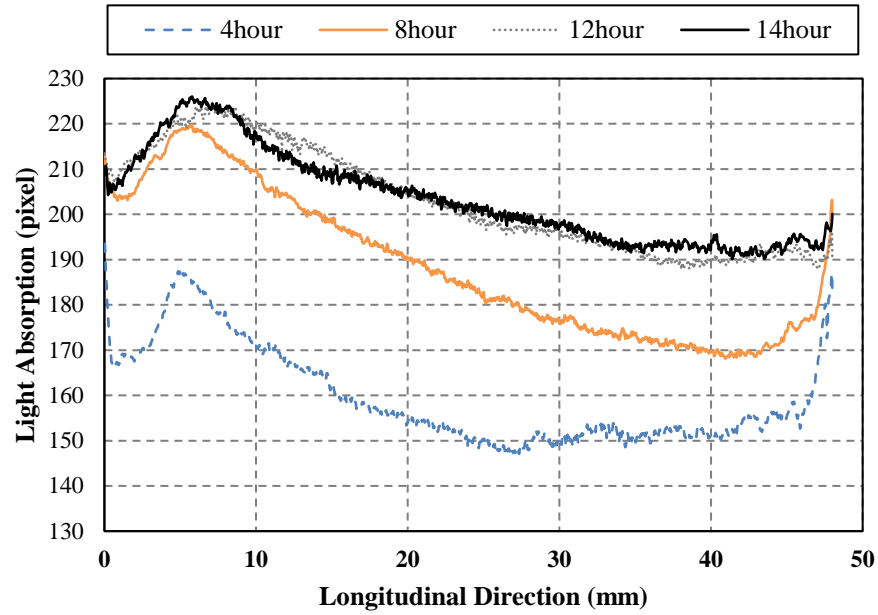


Fig. 12. Asphaltene deposition along longitudinal direction in terms of different elapsed time experiment

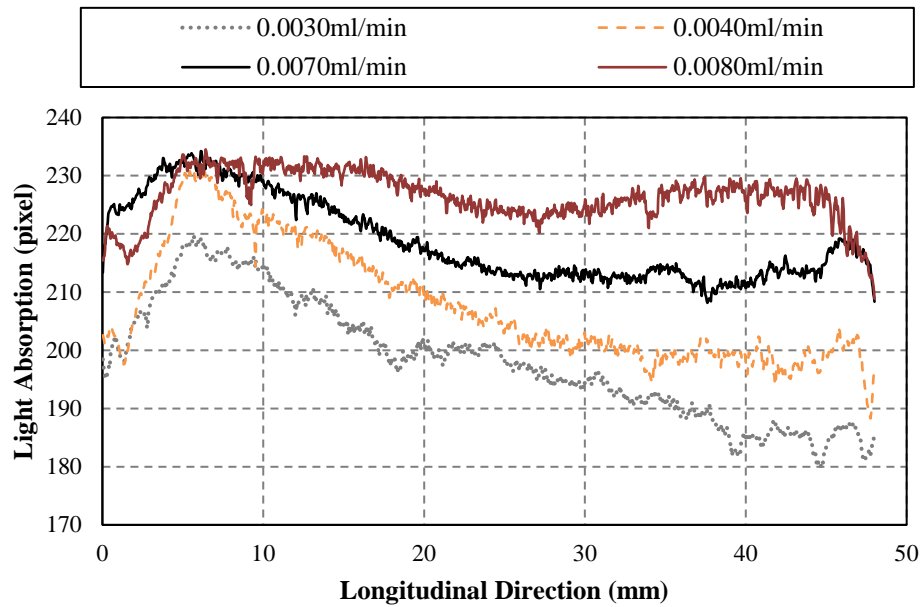


Fig. 13. Asphaltene deposition along longitudinal direction in terms of different flow rate experiments

The results described above show that asphaltene deposition decreases with increasing longitudinal distance from the inlet. There is a maximum deposition point in all experimental curves and this point is located around 5 mm longitudinal distance. However, under a different experimental condition, the range of light absorption is different.

In this work, asphaltene deposition along the longitudinal direction was found to be nonuniform. Deposition decreases with increasing longitudinal distance from the inlet. Nonuniform asphaltene deposition can also be found in the works of Wang *et al.*^[8], Hoepfner *et al.*^[10], and Boek *et al.*^[12] All of them were using capillary tubes for experiments. Wang *et al.*^[8] utilized stainless steel capillary tubes (1600 to 3200 mm length and 6.096 mm internal diameter) while Hoepfner *et al.*^[10] used a 50 mm length and 9.144 mm internal diameter capillary. Boek *et al.*^[12] used a rectangular capillary (100 mm × 600 μm × 150 μm = length × width × depth).

Nonuniform distribution of asphaltene deposition along longitudinal direction can be explained as follows:^[10]

- 1) Local mass transport limitations. This can be explained by the Sherwood number and mass transfer coefficient. Sherwood number stands for the ratio of convective to diffusive mass transport (Equation 7). Convective mass transport is dependent on mass transfer coefficient while diffusive mass transport relies on the size of asphaltene aggregates. Mass transfer coefficient is a function of longitudinal direction and decreases with increasing longitudinal distance from the inlet.^[23] Therefore, Sherwood number has a maximum value near the entrance and declines with increasing longitudinal distance until the region where it is independent of the longitudinal distance. This region is called the fully developed region.

$$Sh = \frac{\text{Convective transport}}{\text{Diffusive transport}} = \frac{k_m L}{D} \quad (7)$$

- 2) Asphaltene aggregation size effect. This should be decided by calculated residence time.

From the calculations, the residence time for these experimental conditions ranges from 9 s ($Q_{oil} = 0.05$ ml/min) to 150 s ($Q_{oil} = 0.003$ ml/min). It is possible to affect the asphaltene aggregation size since the maximal residence time can be up to 150 s.

- 3) Depletion effect. With increasing of longitudinal distance, asphaltene particles deposit and the amount of asphaltene particles in the mixture reduces. This is called the depletion effect which is also related to the capture efficiency. Capture efficiency is dependent on the quantity of deposited insoluble asphaltene and the total insoluble asphaltene. For the experiment of 0.005 ml/min and 10 hours using A crude oil (ratio of oil to n-C7 = 3:7), the total injection asphaltene is near 100 mg and the deposition quantity is just 14 mg. Therefore, the calculated capture efficiency is 14%. For all experiments, the capture efficiency is less than 20% and therefore the deposition distributions are not affected by depletion effect.

- 4) Gravity effect. All experiments were conducted using the vertical configuration, the gravity effect should be taken into account. Through the calculation using the equation 8,^[16] the calculated gravity number is smaller than 0.001. Therefore, the gravity effect is not important.

$$G = \frac{(\rho_a - \rho)gAr^2}{18\mu Q_T} \quad (8)$$

Therefore, in this study, causes of non-uniform deposition distribution are due to local mass transport limitations and asphaltene aggregation size effect.

4. Conclusions

In this study, experiments in microchannel were carried out to investigate asphaltene deposition in terms of the ratio of fluid mixture (crude oil and n-heptane), elapsed time, flow rate and injection volume of crude oil. A non-intrusive measurement technique based on light absorption and image processing is employed to investigate the asphaltene deposition in a transparent micro-channel.

Experimental results show that asphaltene deposition process might follow three stages, (i) small asphaltene particle deposition at the beginning of the experiment, (ii) a rapid and continuous asphaltene deposition increase after few hours and (iii) a decrease on deposition rate in the system at the end of the experimentation. The experimental results in terms of different mixing ratios illustrate that deposits increase with the increasing of the concentration of n-heptane.

Experiments regarding injection volume of crude oil were studied. Two conditions were applied, consisting of time dependent and flow rate dependent asphaltene deposition experiments. Results show that continuous asphaltene deposition can be represented by light absorption in terms of the elapsed time. An empirically fitted curve in logarithmic trend is plotted and can be used for validation of numerical simulations. As for experiments using different flow rates at constant injection time, a logarithmic function was obtained. Combining these two experimental data, the relation between normalized light absorption and the injection volume of crude oil was found.

Shear rate dependent asphaltene deposition experiments in microchannel were performed at constant injection volume and varying flow rate of crude oil. It is found that asphaltene deposition reflected by normalized light absorption reduces with increasing flow rate. The

increase of flow rate leads to the reduction of residence time. It also shows the effect of shear forces on the asphaltene deposition since increasing flow rate leads to a higher shear rate.

Asphaltene deposition along the longitudinal direction is not uniform. Deposits decrease with increasing longitudinal distance from the inlet. This non-uniform deposition distribution is due to local mass transport limitations and asphaltene aggregation size effect.

Author Information

*Phone: +971-26075 396. E-mail: agoharzadeh@pi.ac.ae

Acknowledgments

The work is supported by a research Grant (RD006) from Abu Dhabi National Oil Company (ADNOC) through the Oil Sub- Committee.

List of Abbreviations/Notations

| | |
|-------|---|
| a | Half of microchannel depth (m) |
| A | Cross-sectional area (m ²) |
| b | Half of microchannel width (m) |
| D | Diffusion constant (m ² /s) |
| G | Gravity number |
| I | Normalized light absorption |
| I^* | Normalized light absorption for longitudinal analysis |
| k_m | Mass transfer coefficient (m/s) |
| L | Characteristic length (m) |
| Q | Flow rate (m ³ /s) |
| r | Radius of the spherical particle (m) |

| | |
|--------------------|---|
| Sh | Sherwood number |
| t | Elapsed time (s) |
| v | Average flow velocity (m/s) |
| V | Injection volume (m ³) |
| x^* | Normalized longitudinal distance |
| δ | Thickness of asphaltene deposits (m) |
| ρ | Effective density of the fluid (kg/m ³) |
| ρ_a | Density of asphaltene (kg/m ³) |
| $\gamma_{average}$ | Average shear rate (s ⁻¹) |

References

- [1] Papadimitriou, N., Romanos, G., Charalambopoulou, G. C., Kainourgiakis, M., Katsaros, F., and Stubos, A. (2007) *J. Petrol. Sci. Eng.*, 57:281-293.
- [2] Gonzalez, D. L., Ting, P.D., Hirasaki, G. J., Chapman, W.G. (2005) *Energ. Fuel*, 19: 1230-1234,
- [3] Adebisi, F., and Thoss, V. (2014) *Fuel*, 118: 426-431.
- [4] Creek, J. L. (2005) *Energ. Fuel.*, 19: 1212-1224.
- [5] Buckley, J. S. (2012) *Energ. Fuel.*, 26: 4086-4090.
- [6] Arsalan, N., Palayangoda, S. S., and Nguyen, Q. P., (2014) *J. Petrol. Sci. Eng.*, 121: 66-77.
- [7] Broseta, D., Robin, M., Savvidis, T., Féjean, C., Durandau, M., and Zhou, H., (2000) SPE/DOE Improved Oil Recovery Symposium. Society of Petroleum Engineers. SPE-59294-MS.
- [8] Wang, J., Buckley, J. S., and Creek, J. L. (2004) *J. Dispersion Sci. Technol.*, 25: 287-298.

- [9] Nabzar, L. and Aguiléra, M. (2008) *Oil & Gas Science and Technology-Revue de l'IFP*, 63: 21-35.
- [10] Hoepfner, M.P., Limsakoune, V., Chuenmeechao, V., Maqbool, T., and Fogler, H.S. (2013) *Energ. Fuel.*, 27: 725–735.
- [11] Seifried, C.M., Al Lawati, S., Crawshaw, J.P., and Boek, E.S. (2013) Society of Petroleum Engineers, SPE 166289.
- [12] Boek, E. S., Ladva, H. K., Crawshaw, J. P., and Padding, J. T. (2008) *Energ. Fuel.*, 22: 805-813.
- [13] Boek, E. S., Wilson, A. D., Padding, J. T., Headen, T. F., and Crawshaw, J. P. (2009) *Energ. Fuel.*, 24: 2361-2368.
- [14] Boek, E. S., Seifried, C. M., Crawshaw, J. P., and Al Lawati, S. (2013) *SPE ATCE*, New Orleans, Louisiana, USA, 30 September-2 October,. SPE-166289-MS.
- [15] Dehghan, A. A., Farzaneh, S. A., Kharrat, R., Ghazanfari, M. H., and Rashtchian, D. (2010) *Transport Porous Med.*, 83: 653–666.
- [16] Lawal, K. A., Crawshaw, J. P., Boek, E. S., and Vesovic, V. (2012) *Energ. Fuel.*, 26: 2145-2153.
- [17] Hu, C., Morris, J. E., and Hartman, R. L. (2014) *Lab Chip*, 14: 2014-2022.
- [18] Doryani, H., Malayeri, M.R. and Riazi, M. (2016) *Fuel*, 182: 613–622,
- [19] Lin, Y.J., He, P., Tavakkoli, M., Mathew, N.T. Fatt, Y.Y., Chai, J.C., Goharzadeh, A., Vargas, F.M. and Biswal S.L. (2016) *Langmuir*, 32: 8729–8734.
- [20] Zanganeh, P., Dashti, H., Ayatollahi S, (2015) *Fuel*, 160:132-139
- [21] Zhuang, Y., Goharzadeh, A., Lin, Y.J., Yap, Y.F., Chai, J.C., Mathew N., Vargas F., Biswal S. L. (2016) *J. Petrol. Sc. Eng.*, 45: 77–82.

[22] Ladva, H. K., Wilson, A., Crawshaw, J., Boek, E., and Padding, J. (2009) in *SPE EFDC*, Scheveningen, The Netherlands, 27-29 May, SPE-122197-MS.

[23] Incropera, F. P., *Fundamentals of heat and mass transfer* (2011) John Wiley & Sons.